Lumen Mass Transfer in Hollow-Fiber Membrane Processes with Constant External Resistances

Yingjie Qin and Joaquim M. S. Cabral
Laboratório de Engenharia Bioquímica, Centro de Engenharia Biológica e Química, Instituto Superior Técnico, 1000 Lisboa, Portugal

Hollow-fiber membrane processes with a constant external resistance having a constant or variable shell concentration resulting from an operational mode of cocurrent or countercurrent are studied. By solving numerically the continuity mass-conservation equation with the corresponding boundary conditions, the lumen laminar mass-transfer coefficients for both cases are correlated. The correlations greatly improve the calculating accuracy of the overall mass-transfer coefficient and can be used to obtain the lumen mixed-cup concentration by an algebraic equation substituting the partial differential equation. A separation factor m′ is introduced to characterize the effect of the operational mode. Calculation results demonstrate that the lumen mass-transfer coefficient is independent of the real lumen and shell concentrations, but it is greatly influenced by m′. The countercurrent mode, compared to the cocurrent mode, provides not only a higher mean driving force, but a higher lumen mass-transfer coefficient. This conclusion is novel and valid for the tube-shell heat or mass-transfer processes and is supported by the experimental data in the literature and our gas membrane separation experiments.

Introduction

Membrane processes have recently become an accepted unit operation for a wide variety of separations in industry and in environmental applications. Because of the high surface area per unit volume and the other advantages, hollow-fiber modules have been found almost in all branches of membrane applications. Among them are the cases in which the membrane-permeating component is diluted in the lumen fluid, and they can be found in new membrane processes under development, such as membrane-based extraction (MBE), the supported liquid membrane (SLM) process, the hollow-fiber-contained liquid membrane (HFCLM) process, the supported gas membrane (SGM) process, membrane-based absorption/desorption (MBAD) (similar to the SGM process, but the micropores are wetted by the liquid phase), permabsorption, membrane gas (vapor) permeation, pervaporation, perstraction, membrane reactor, as well as in dialysis, a more traditional application. In these cases, the flux through the membrane is small, and thus the volumetric flow rates of the two fluids, unlike in the traditional pressure-driven membrane processes such as reverse osmosis, ultrafiltration, and microfiltration, can be taken as constant. Due to the low concentration of the membrane-permeating component, its phase partition coefficient and its diffusion coefficient in the membrane and the shell fluid can be taken as constants (Prasad and Sirkar, 1990; Yun et al., 1992; Urtiaga et al., 1992; Tompkins et al., 1992; Hutter et al., 1994; Brookes and Livingston, 1995; Qin et al., 1996); therefore, the membrane wall and shell resistances are concentration independent. When the shell resistance is length independent (Wang et al., 1992; Costello et al., 1993), the combined mass-transfer coefficient from the wall and shell is constant, and it is described as the external mass-transfer coefficient (Qin and Cabral, 1996). Mathematical models for hollow-fiber (or other tubular-mass or heat-transfer) processes have been adopted by considering the velocity and concentration profiles along the hollow fiber by means of the continuity mass-conservation equation and the associated boundary conditions. When external resistance and shell concentration are constant (called Case A), analytical solutions are available (Kooijman, 1973; Cooney et al., 1974). Numerical methods

Correspondence concerning this article should be addressed to J. M. S. Cabral.

have been used to solve the same problem for membrane processes (Tang and Hwang, 1976; Raghunath and Hwang, 1992; Kreulen et al., 1993; Karoor and Sirkar, 1993; Wang et al., 1993; Qin et al., 1996).

However, Case A, which demands a constant shell concentration, does not occur frequently in industrial practice, except for a few examples: (1) a component is instantaneously reactively absorbed (or extracted) from the feed in the lumen through the membrane wall to a solution in the shell (Zhang and Cussler, 1985a,b; Nii et al., 1992; Wang et al., 1993; Urtiaga and Irabien, 1993; Qin et al., 1996); (2) the pure gas in the shell is physically absorbed by a fluid in the lumen through a wetted or unwetted porous wall (Karoor and Sirkar, 1993; Kreulen et al., 1993); (3) the shell is kept under vacuum (Raghunath and Hwang, 1992); (4) when the fluid flow in the shell is in excess or/and the phase distribution coefficient is small (Cooney et al., 1974; Prasad and Sirkar, 1988; Hutter et al., 1994); and (5) when a first-order reaction occurs at the wall (Wu et al., 1993; Yi and Tavlarides, 1995 (see the Appendix)). Nevertheless, this limit case is most frequently explored in experimental measurements of the membrane mass-transfer coefficient and provides an easy way to understand the mass-transfer mechanisms.

Chemical engineers have tried to avoid the complexity of solving partial differential equations, especially for the purpose of design. Many researchers have assumed plug-flow and lumped lumen mass-transfer effects into a film-type mass transfer coefficient to describe lumen mass transfer. The correlations of the lumen mass-transfer coefficient of the Leveque equation type, or Skelland's solution of Graetz problem are used in almost all hollow-fiber membrane applications, such as the MBE process (D'Elia et al., 1986; Dahuron and Cussler, 1988; Prasad and Sirkar, 1988; Takeuchi et al., 1990; Tompkins et al., 1992; Yun et al., 1992; Hutter et al., 1994; Yeh and Huang, 1995), the SGM process (Zhang and Cussler, 1985a,b; Yang and Cussler, 1986; Wang and Cussler, 1992; Karoor Sirkar, 1993; Tai et al., 1994), the MBAD process (Karoor and Sirkar, 1993; Hutter et al., 1994), the SLM process (Takeuchi et al., 1990; Urtiaga and Irabien, 1993), the HFCLM process (Basu and Sirkar, 1992), membrane distillation (Sarti et al., 1993), permabsorption (Nii et al., 1992; Al-Saffar et al., 1995), membrane gas (vapor) permeation (Wang et al., 1992), pervaporation (Raghunath and Hwang, 1992), perstraction (Brookes and Livingston, 1995), membrane adsorption (Saito et al., 1988), and hollow-fiber bioreactor (Wu et al., 1993), as well as the dialysis, reverse osmosis, and ultrafiltration processes.

However, the availability of simple but accurate correlations is limited. For instance, the Leveque equation and Skelland's solution of the Graetz problem (Prasad and Sirkar, 1988) are only strictly valid for the case of a constant lumen wall concentration and the concentration profile rarely developed. Urtiaga and Irabien (1993) suggested a correlation for the SLM process (Case A), neglecting the effect of Sh_w. Nevertheless, as concluded from the analytical and numerical solutions (Kooijman, 1973; Qin et al., 1996), the lumen Sherwood number is a function of Sh_w and the Graetz number, G_z. However, since the early correlations for the lumen mass-transfer coefficient (Yang and Cussler, 1986; Dahuron and Cussler, 1988; Prasad and Sirkar, 1988), not many more correlations have been suggested (Takeuchi et al., 1990; Urtiaga and Irabien, 1993). Apparently, researchers have recently paid more attention to the shell mass-transfer coefficient (Takeuchi et al., 1990; Nii et al., 1992; Wang et al., 1992; Costello et al., 1993).

In many experimental cases and industrial applications, hollow-fiber processes may be carried out under conditions where both the lumen and shell concentrations change significantly. Thus the concentration fields in the lumen, membrane wall, and shell are coupled through mutual boundary conditions at the interfaces, and the problem should be treated as a coupled boundary problem (Yi and Tavlarides, 1995). On the other hand, many researchers still use correlations like the Leveque equation to obtain the lumen mass-transfer coefficient for this case (D'Elia et al., 1986; Dahuron and Cussler, 1988; Yun et al., 1992; Hutter et al., 1994; Yeh and Huang, 1995). Will the axial variation of the shell concentration greatly influence the lumen-mass transfer coefficient, and if so, how will it? However, no theoretical analysis or intended experimental performance have been reported.

In this study, numerical simulations are performed to calculate the lumen Sherwood number for Case A, and for the case when Sh_w is constant while the shell concentration varies along the axial direction, resulting from the cocurrent or countercurrent operation mode (Case B). Empirical but accurate correlations of the lumen Sherwood number are provided for a wide range of Sh_w and G_z for both cases.

SGM absorption/desorption experiments are performed to examine the influence of cocurrent and countercurrent modes on the lumen Sherwood number.

Theory

Mass-transfer model for Case A

The following assumptions are made to describe the fluid flow and the transport of a single component in the lumen of hollow fibers and the transport at the lumen interface: (1) the fluid in the lumen of the fibers is Newtonian and has constant physical properties; (2) no source or sinks exist in the lumen; (3) fluid flow through the lumen of fibers is a steady laminar flow, valid in most cases for hollow-fiber processes with low pressure drops; (4) the flow rate in the lumen is constant along the fiber axis, and is valid when the concentration of the component in the lumen is diluted; (5) due to the unique configuration of the hollow-fiber modules that the fibers are usually epoxy bonded to the ends of the shell, the laminar flow in the lumen is fully developed when the mass transport through the lumen interface occurs at a certain distance from the module entrance; (6) radial transfer of the component in the lumen is by Fickian diffusion, radial convection is neglected, and axial diffusion is neglected compared to axial convection; (7) the component partition coefficient at phase interface(s) is constant; (8) resistance of the membrane and the shell fluid are unchanged with the axial direction; and (9) bulk concentration of the component in the shell side is treated the same as the axial direction.

Therefore the concentration profiles in the lumen can be established as

$$2u\left[1-\left(\frac{r}{R}\right)^2\right]\frac{\partial C}{\partial z}=D\left[\frac{1}{r}\frac{\partial}{\partial r}\left(r\frac{\partial C}{\partial r}\right)\right], \qquad (1)$$

with the following boundary conditions (BC):

$$\text{BC1: } C = C_0,\ z = 0, \text{ for all } r \tag{2}$$

$$\text{BC2: } \frac{\partial C}{\partial r} = 0,\ r = 0, \text{ for all } z \tag{3}$$

$$\text{BC3: } D\frac{\partial C}{\partial r} = -K(C_R - mC_s),\ r = R, \text{ for all } z. \tag{4}$$

The membrane processes covered in this article fall into one of four basic categories:

Type I: there is no phase interface at the lumen-side and outside surfaces of the hollow-fiber membrane, for instance, dialysis;

Type II: there is a phase interface at the lumen-side surface, for instance, the SGM, MBE, or MBAD process, when the porous membrane is wetted by the shell phase;

Type III: there is a phase interface at the shell-side surface, for instance, the SGM, MBE, or MBAD process, when the porous membrane is wetted by the lumen phase;

Type IV: there are two phase interfaces at the lumen-side and shell-side surfaces, respectively, for instance, the SGM or SLM process, where the porous membrane is impregnated by the third (gas or liquid) phase, or pervaporation, gas (vapor) permeation, permabsorption, perstraction process, where a nonporous membrane is used.

Therefore, the third boundary condition at the membrane wall can be further expressed as

$$-D\frac{\partial C}{\partial r} = k_m(C_R - C_{m,s}) = k_s(C_{m,s} - C_s) \quad \text{(Type I)} \tag{5a}$$

$$-D\frac{\partial C}{\partial r} = k_m\left(\frac{C_R}{m_l} - C_{m,s}\right) = k_s(C_{m,s} - C_s) \quad \text{(Type II)} \tag{5b}$$

$$-D\frac{\partial C}{\partial r} = k_m(C_R - m_sC_{m,s}) = k_s(C_{m,s} - C_s) \quad \text{(Type III)} \tag{5c}$$

$$-D\frac{\partial C}{\partial r} = k_m\left(\frac{C_R}{m_l} - m_sC_{m,s}\right) = k_s(C_{m,s} - C_s) \quad \text{(Type IV).} \tag{5d}$$

Equations (5a–5d) can be further arranged as

$$-D\frac{\partial C}{\partial r} = \frac{C_R - C_s}{\frac{1}{k_m} + \frac{1}{k_s}} \quad \text{(Type I)} \tag{6a}$$

$$-D\frac{\partial C}{\partial r} = \frac{C_R - m_lC_s}{\frac{m_l}{k_m} + \frac{m_l}{k_s}} \quad \text{(Type II)} \tag{6b}$$

$$-D\frac{\partial C}{\partial r} = \frac{C_R - m_sC_s}{\frac{1}{k_m} + \frac{m_s}{k_s}} \quad \text{(Type III)} \tag{6c}$$

$$-D\frac{\partial C}{\partial r} = \frac{C_R - m_lm_sC_s}{\frac{m_l}{k_m} + \frac{m_lm_s}{k_s}} \quad \text{(Type IV)} \tag{6d}$$

Therefore, BC3 can be used to describe these four cases if:

$$m = 1 \qquad \frac{1}{K} = \frac{1}{k_m} + \frac{1}{k_s} \quad \text{(Type I)} \tag{7a}$$

$$m = m_l \qquad \frac{1}{K} = \frac{m_l}{k_m} + \frac{m_l}{k_s} \quad \text{(Type II)} \tag{7b}$$

$$m = m_s \qquad \frac{1}{K} = \frac{1}{k_m} + \frac{m_s}{k_s} \quad \text{(Type III)} \tag{7c}$$

$$m = m_lm_s \qquad \frac{1}{K} = \frac{m_l}{k_m} + \frac{m_lm_s}{k_s} \quad \text{(Type IV).} \tag{7d}$$

Assuming that

$$r' = r/R \tag{8}$$

$$C' = (C - mC_s)/(C_0 - mC_s) \tag{9}$$

$$z' = zD/4uR^2 = G_z^{-1} \tag{10}$$

$$Sh_w = 2KR/D. \tag{11}$$

Then Eqs. 1–4 can be reduced to the following nondimensional forms:

$$(1 - r'^2)\frac{\partial C'}{\partial z'} = \frac{2}{r'}\frac{\partial}{\partial r'}\left(r'\frac{\partial C'}{\partial r'}\right) \tag{12}$$

$$z' = 0, \qquad C' = 1 \tag{13}$$

$$r' = 0, \qquad \frac{\partial C'}{\partial r'} = 0 \tag{14}$$

$$r' = 1, \qquad \frac{\partial C'}{\partial r'} = -\frac{Sh_w}{2}C'. \tag{15}$$

Membrane processes that can be described by the preceding model are listed in Table 1.

The preceding Fourier-Poisson equation can be solved analytically by separation of variables (Kooijman, 1973; Cooney et al., 1974). In order to stay consistent with the solving models with more complicated boundaries in the following section, the orthogonal collocation method on finite elements in

Table 1. Various Boundary Conditions at the Hollow-Fiber Wall

No.	Boundary Condition at $r = R$	Operation Mode	Researchers
1	$C'_R = 0$	SGM*	Karoor and Sirkar, 1993; Kreulen et al., 1993
2	$\frac{\partial C'}{\partial r'} = \text{constant}$	SLM	Qin and Cabral, 1996
3	$\frac{\partial C'}{\partial r'} = -\frac{Sh_w}{2} C'_R$	SGM	Zhang and Cussler, 1985a,b; Yang and Cussler, 1986; Kreulen et al., 1993; Karoor and Sirkar, 1993; Wang et al., 1993; Costello et al., 1993; Qin et al., 1996
		SLM	Haan et al.,** 1989; Takeuchi et al., 1990; Urtiaga et al., 1992; Urtiaga and Irabien, 1993
		MBE	Takeuchi et al., 1990; Yun et al., 1992; Yi and Tavlarides, 1995**
		MBAD dialyzer	Karoor and Sirkar, 1993† and Kooijman, 1973; Cooney et al., 1974
		permabsorption	Tang and Hwang, 1976; Nii et al., 1992
		gas (vapor) permeation††	Li et al., 1990; Wang et al., 1992
		pervaporation	Raghunath and Hwang, 1992
		perstraction	Brookes and Livingston, 1995
		MD	Salti, 1993
		HFCLM	Basu and Sirkar, 1992
		HF Bioreactor	Kim and Cooney, 1976; Wu et al., 1993
4	$\frac{\partial C'}{\partial r'} = -\frac{Sh_w}{2}[C'_R + m'(C'_z - 1)]$	SGM	Zhang and Cussler, 1985a; Yang and Cussler, 1986; Karoor and Sirkar, 1993; Tai et al., 1994
		MBAD	Karoor and Sirkar, 1993; Hutter et al., 1994
		MBE	D'Elia et al., 1986; Prasad and Sirkar, 1986; Dahuron and Cussler, 1988; Yun et al., 1992; Hutter et al., 1994; Yeh and Huang, 1995
		SLM	Yi and Tavlarides, 1995
		gas permeation††	Li et al., 1990; Wang et al., 1992

* A pure gas in shell absorbed through the unwetted wall to the aqueous phase in lumen.
** The one-order interfacial reaction kinetics is included, see Appendix.
† A pure gas in shell absorbed through the wetted wall to the aqueous phase in lumen.
†† More conventional examples are the removal of VOCs from air.

the r' direction was applied to convert the partial differential equation into a set of coupled ordinary differential equations. The method yields C' at any point within the lumen or on the lumen surface of the hollow fiber by solving these equations in the z'-direction by the Runge-Kutta method (Finlayson, 1980). Other interesting values—the dimensionless mixed cup concentration, C'_z, the local lumen Sherwood number, Sh_z, and the local overall Sherwood number, $Sh_{z,0}$, at any z'—can be obtained as follows (Qin et al., 1996):

$$C'_z = \frac{C_z - mC_s}{C_0 - mC_s} = 4\int_0^1 (1 - r'^2) r' C'\, dr' \tag{16}$$

$$Sh_z = \frac{2RK_z}{D} = -2\frac{\left.\frac{\partial C'}{\partial r'}\right|_{r'=1}}{C'_z - C'_R} = Sh_w \frac{C'_R}{C'_z - C'_R} \tag{17}$$

$$Sh_{z,0} = \frac{2RK_{z,0}}{D} = -2\frac{\left.\frac{\partial C'}{\partial r'}\right|_{r'=1}}{C'_z} = Sh_w \frac{C'_R}{C'_z}. \tag{18}$$

An equivalent expression of Eqs. 17 and 18 can be obtained from additivity of resistances:

$$\frac{1}{Sh_{z,0}} = \frac{1}{Sh_w} + \frac{1}{Sh_z}. \tag{19}$$

For design purposes, uniform velocity and concentration distributions are usually assumed and the average overall mass-transfer coefficient, $K_{\text{avg},z,0}$ is used to characterize the overall transport resistance. If dimensionless variables and parameters are adopted, then the logarithmic averaged overall Sherwood number, $Sh_{\text{avg}z,0}$, and the logarithmic averaged lumen Sherwood number, $Sh_{\text{avg},z}$, can be expressed as (Kooijman, 1973):

$$Sh_{\text{avg},z,0} = -\frac{\ln(C'_z)}{4z'} \tag{20}$$

$$Sh_{\text{avg},z} = 1/(1/Sh_{\text{avg},z,0} - 1/Sh_w). \tag{21}$$

Mass transfer model for Case B

When the fluid in the shell is in parallel flow (cocurrent or countercurrent) and its concentration variation is not negligible, assumptions (1–8) are still valid to describe the fluid flow and the mass transport in the lumen and the transport at the lumen interface, but assumption (9) is omitted. Therefore, the partial differential equation and boundary conditions, Eqs. 1–4, are still valid. Nevertheless, C_s in BC3 will vary along the z-direction. By macroscopic mass balance, BC3 can be reexpressed as

$$D\frac{\partial C}{\partial r} = -K(C_R - mC_{s,z}) = -K\left[C_R - m\frac{Q_l}{Q_s}(C_0 - C_z) - mC_s^*\right] \quad \text{(cocurrent)} \quad (22)$$

$$D\frac{\partial C}{\partial r} = -K(C_R - mC_{s,z}) = -K\left[C_R + m\frac{Q_l}{Q_s}(C_0 - C_z) - mC_s^*\right] \quad \text{(countercurrent)}, \quad (23)$$

where C_s^* is the bulk shell concentration at the module end where the lumen fluid enters whether the operation is in co- or countercurrent mode, and mQ_l/Q_s is defined as a separation factor such as an absorption (extraction) or stripping factor, as in the convenient absorption/desorption or extraction/stripping process (Perry and Green, 1984). Assuming

$$C' = (C - mC_s^*)/(C_0 - mC_s^*) \quad (24)$$

$$m' = mQ_l/Q_s \quad \text{(cocurrent)} \quad (25)$$

$$m' = mQ_l/Q_s \quad \text{(countercurrent)}, \quad (26)$$

the boundary condition at the fiber wall can be made dimensionless:

$$\frac{\partial C'}{\partial r'} = -\frac{Sh_w}{2}[C' + m'(C'_z - 1)] \qquad r' = 1, \quad \text{for all } z', \quad (27)$$

where C'_z is the dimensionless mixed-cup lumen concentration, as defined by Eq. 16, but in which C_s is replaced by C_s^*. It must be noted that Eq. 27 is right for both cases of cocurrent and countercurrent, positive values of m' denote cocurrent, and negative values of m' denote countercurrent.

Equations 12–14 and 27 can be solved by the orthogonal collocation method on finite elements, as described for Case A. By using the orthogonal collocation method, C'_z can be expressed as a linear function of the dimensionless concentration on collocation points (Finlayson, 1980), hence substituting Eq. 27 for Eq. 15 does not create more difficulties for solving the equations. Thus, whether for the cocurrent or countercurrent mode, for a value of C'_z obtained as a function of Sh_w, $m'$and z', two of the four real concentrations, C_0, C_z, $C_{s,0}$, and $C_{s,z}$, can be calculated if two of them are given by solving Eq. 24 and the mass balance equation, which is discussed in another article (Qin and Cabral, 1997). Also, Sh_z and $Sh_{z,0}$ can be calculated as follows:

$$Sh_z = \frac{2RK_z}{D} = -2\frac{\left.\frac{\partial C'}{\partial r'}\right|_{r'=1}}{C'_z - C'_R} = Sh_w\frac{C'_R + m'(C'_z - 1)}{C'_z - C'_R} \quad (28)$$

$$Sh_{z,0} = \frac{2RK_{z,0}}{D} = -2\frac{\left.\frac{\partial C'}{\partial r'}\right|_{r'=1}}{C'_z} = Sh_w\frac{C'_R + m'(C'_z - 1)}{C'_z}. \quad (29)$$

By macroscopic mass balance, $K_{\text{avg},z,0}$ can also be calculated as

$$K_{\text{avg},z,0} = -\frac{Ru}{2z}\frac{\ln\dfrac{C_z - mC_{s,z}}{C_0 - mC_{s,0}}}{\left(1 + m\dfrac{Q_l}{Q_s}\right)} \quad \text{(cocurrent)} \quad (30)$$

$$K_{\text{avg},z,0} = -\frac{Ru}{2z}\frac{\ln\dfrac{C_z - mC_{s,0}}{C_0 - mC_{s,z}}}{\left(1 - m\dfrac{Q_l}{Q_s}\right)} \quad \text{(countercurrent)} \quad (31)$$

$$K_{\text{avg},z,0} = \frac{Ru}{2z}\frac{C_0 - C_z}{C_0 - mC_{s,z}} \quad \text{(countercurrent, } m' = -1\text{)}. \quad (32)$$

Expressing Eqs. 30–32 in the form of a dimensionless concentration leads to

$$Sh_{\text{avg},z,0} = -\frac{\ln[C'(1+m') - m']}{4(1+m')z'} \quad \text{(when } m' \neq -1\text{)} \quad (33)$$

$$Sh_{\text{avg},z,0} = \frac{1 - C'}{4z'} \quad \text{(when } m' = -1\text{)}. \quad (34)$$

When $m' = 0$, Eqs. 28, 29 and 33 are reduced to Eqs. 17, 18 and 20, respectively. $Sh_{\text{avg},z}$ can be obtained by using Eq. 21. As can be seen from Eqs. 12–16 and 27, C'_z is a function of z', Sh_w, and m', independent of values of C_0 and C_s^*. Thus, Sh_z, $Sh_{z,0}$, $Sh_{\text{avg},0}$, $Sh_{\text{avg},z,0}$ and $K_{\text{avg},z,0}$ are a function of z', Sh_w, and m', but independent of C_0 and C_s^*. From Eqs. 30–32, mixed-cup concentration in the lumen outlet can be expressed as

$$C_Z = \frac{C_0\left\{m\dfrac{Q_l}{Q_s} + \exp\left[-\dfrac{2ZK_{\text{avg},Z,0}}{Ru}\left(1 + m\dfrac{Q_l}{Q_s}\right)\right]\right\} + mC_{s,0}\left\{1 - \exp\left[-\dfrac{2ZK_{\text{avg},Z,0}}{Ru}\left(1 + m\dfrac{Q_l}{Q_s}\right)\right]\right\}}{1 + m\dfrac{Q_l}{Q_s}} \quad \text{(cocurrent)} \quad (35)$$

$$C_Z = \frac{C_0\left(1 - m\frac{Q_l}{Q_s}\right)\exp\left[-\frac{2ZK_{\text{avg},Z,0}}{Ru}\left(1 - m\frac{Q_l}{Q_s}\right)\right] + mC_{s,0}\left\{1 - \exp\left[-\frac{2ZK_{\text{avg},Z,0}}{Ru}\left(1 - m\frac{Q_l}{Q_s}\right)\right]\right\}}{1 - m\frac{Q_l}{Q_s}\exp\left[-\frac{2ZK_{\text{avg},Z,0}}{Ru}\left(1 - m\frac{Q_l}{Q_s}\right)\right]} \quad \text{(countercurrent)} \quad (36)$$

$$C_Z = \frac{C_0 + mC_{S,0}\dfrac{2ZK_{\text{avg},Z,0}}{Ru}}{1 + \dfrac{2ZK_{\text{avg},Z,0}}{Ru}}. \quad \text{(countercurrent, } mQ_l/Q_s = 1) \quad (37)$$

If the fluids in the lumen and shell are recycled between the reservoirs and the hollow-fiber module, respectively, and the holdup effect resulting from the pipelines is neglected, then

$$-V_l\frac{dC_0}{dt} = Q_l(C_0 - C_Z) \quad (38)$$

$$-V_s\frac{dC_{s,0}}{dt} = Q_s(C_{s,0} - C_{s,Z}), \quad (39)$$

where V_l and V_s are the total volumes of the fluids recycled in the lumen and shell sides, respectively, which are assumed to remain unchanged during the process; C_Z or $C_{s,Z}$ are the module exit concentration of the lumen and the shell, respectively, corresponding to the inlet concentrations C_0 and $C_{s,0}$ in the same time by a pseudo-steady-state assumption. Integrating Eqs. 38 and 39 combining with Eqs. 35–37 leads to

$$\ln\frac{C_0(0) - mC_{s,0}(0)}{C_0(t) - mC_{s,0}(t)} = \ln\frac{C_0(0) - mC_{s,0}(0)}{C_0(t) - mC_{s,0}(0) - m\dfrac{V_l}{V_s}[C_0(0) - C_0(t)]} = \frac{\dfrac{1}{V_L} + \dfrac{m}{V_s}}{\dfrac{1}{Q_l} + \dfrac{m}{Q_s}}\left\{1 - \exp\left[-\frac{2ZK_{\text{avg},Z,0}}{Ru}\left(1 + m\frac{Q_l}{Q_s}\right)\right]\right\}t$$

$$\text{(cocurrent, } m' > 0) \quad (40)$$

$$\ln\frac{C_0(0) - mC_{s,0}(0)}{C_0(t) - mC_{s,0}(t)} = \ln\frac{C_0(0) - mC_{s,0}(0)}{C_0(t) - mC_{s,0}(0) - m\dfrac{V_l}{V_s}[C_0(0) - C_0(t)]} = \frac{\dfrac{1}{V_1} + \dfrac{m}{V_s}}{\dfrac{1}{Q_l} - \dfrac{m}{Q_s}\exp\left[-\dfrac{2ZK_{\text{avg},Z,0}}{Ru}\left(1 - m\dfrac{Q_l}{Q_s}\right)\right]} \times \left\{1 - \exp\left[-\frac{2ZK_{\text{avg},Z,0}}{Ru}\left(1 - m\frac{Q_l}{Q_s}\right)\right]\right\}t$$

$$\text{(countercurrent, } m' < 0,\ m' \neq -1) \quad (41)$$

$$\ln\frac{C_0(0) - mC_{s,0}(0)}{C_0(t) - mC_{s,0}(t)} = \ln\frac{C_0(0) - mC_{s,0}(0)}{C_0(t) - mC_{s,0}(0) - m\dfrac{V_l}{V_s}[C_0(0) - C_0(t)]} = \frac{\dfrac{2ZK_{\text{avg},Z,0}}{Ru}}{1 + \dfrac{2ZK_{\text{avg},Z,0}}{Ru}}\left(\frac{1}{V_l} + \frac{m}{V_s}\right)Q_l t.$$

$$\text{(countercurrent, } m' = -1). \quad (42)$$

Expressions similar to Eqs. 40 and 41 have been derived from or used for SGM and MBE processes (Zhang and Cussler, 1985; D'Elia et al., 1986; Dahuron and Cussler, 1988; Tai et al., 1994; Yeh and Huang, 1995). Equations 40–42 imply that the logarithm of $C_0(t) - mC_{s,0}(t)$ varies linearly with time. Thus measurements of the difference in concentration between the two reservoirs vs. t (time) allows us to calculate the mass-transfer coefficient $K_{\text{avg},Z,0}$ or $Sh_{\text{avg},Z,0}$ (Yang and Cussler, 1986).

Experimental Studies

Microporous hydrophobic Plasmaphan polypropylene hollow fibers (ID 0.33 mm, wall thickness 0.15 mm, porosity 70%) from Akzo/Enka were used. The desired number of hollow fibers were placed into an external glass shell and glued at both ends of the shell with an epoxy. The characteristics of hollow-fiber modules used in this study are fiber number 90, effective length 0.14 m, shell internal diameter 7.7 mm, and packing density 61%.

Figure 1 shows the experimental setup, and the experimental procedures were previously described (Qin et al., 1996). An aqueous solution (1 L) with the given concentration of NH_3 (ca. 0.1 M) served as the feed. Pure water was used as the stripping solution. In some experiments, a 0.5-M Na_2SO_4 aqueous solution instead of pure water was used as the feed or the stripping solution. Both solutions were contained in a glass vessel with a stirring bar. Temperature was maintained by a water bath within an error of ± 0.1°C. After stirring for several minutes to attain thermal equilibrium, the feed was pumped through the lumen side, and the stripping solution through the shell side in co- or countercurrent mode. Both the feed and stripping solutions were recycled between the module and the reservoirs. Samples of 2 mL were taken from

the feed reservoir at appropriate time intervals, and the concentration of ammonia was determined by titration with 0.02-M HCl using an autotitrator with errors less than 0.3%.

Results and Discussion

Lumen mass-transfer coefficient for Case A

The major difficulty in the analytical solution of Case A is accurately computing the higher eigenvalues and eigenfunctions, if accurate solutions are desired for the entrance region (Cooney et al., 1974). When the method of orthogonal collocation on finite elements was used, more than 40 finite elements in the r'-direction and a value of 2.5×10^{-4} for the size of the finite elements near the wall were required in the entrance region in order to ensure that the relative error of Sh_z was less than 10^{-5}. Fortunately, the size of the finite elements in the r'-direction and the size of the step in the z'-direction can be extended very quickly, as z' increases without influencing the accuracy of Sh_z (relative error $\leq 10^{-5}$). The numerical results were compared with the results calculated by Kooijam (1973) and Worsoe-Schmidt (1967), as in Table 2.

Because the Graetz problem of a constant concentration boundary condition is identical to Case A when $Sh_w = +\infty$, and the problem of a constant flux boundary condition is identical to Case A when $Sh_w = 0$ (Kooijman, 1973), neither of them is discussed further.

Kooijman (1973) pointed out that for many cases the influence of Sh_w on $Sh_{\text{avg},z,0}$ is small, and so $Sh_{\text{avg},z,0}$ can be obtained by simply combining Sh_w with $Sh_{\text{avg},z}$ for a constant concentration boundary condition. This conclusion is still true when Sh_w is extremely high or extremely low. However, the resulting errors increase when Sh_w is in the middle range, characterizing the practical operation [for instance, Sh_w is calculated to be 5.6 for an SGM process (Qin et al., 1996) and to be 12.7 for an SLM process (Urtiaga et al., 1993)]. The

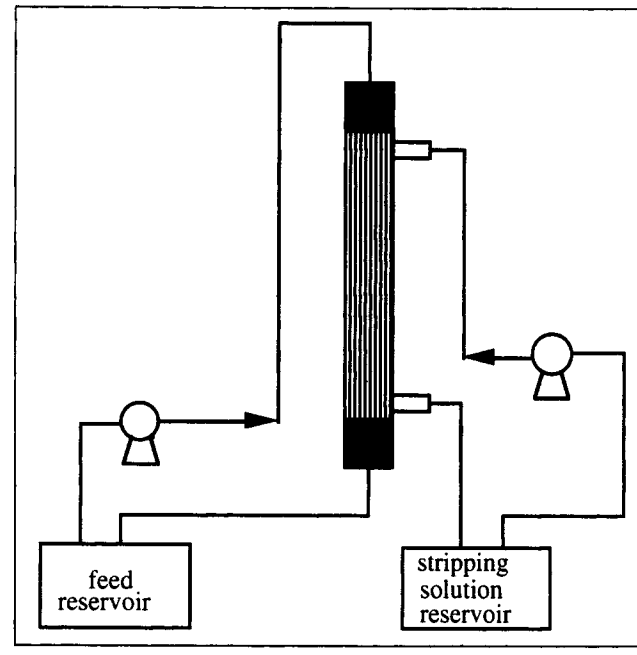

Figure 1. Experimental apparatus.

Table 2. Numerical Results of Sherwood Number vs. Analytical Results

	$Sh_w = +\infty$					$Sh_w = 0$	
z'	Sh_z	Sh_z^*	Sh_z^{**}	$Sh_{\text{avg},z}$	$Sh_{\text{avg},z}^{**}$	Sh_z	Sh_z^{**}
2.5×10^{-5}	35.805		35.806	54.176		43.654	43.651
5.0×10^{-5}	28.254		28.254	42.814		34.510	34.511
1.0×10^{-4}	22.280	22.46	22.278	33.811	33.84	27.275	27.276
2.0×10^{-4}	17.559	17.33		26.684	26.75	21.557	
2.5×10^{-4}	16.264		16.264	24.723		19.987	19.987
4.0×10^{-4}	13.842	13.83		21.049	21.05	17.049	
5.0×10^{-4}	12.824		12.824	19.501		15.814	15.813
7.0×10^{-4}	11.433	11.43		17.379	17.38	14.123	
1.0×10^{-3}	10.131	10.13	10.130	15.384	15.38	12.539	12.538
2.0×10^{-3}	8.0363	8.036		12.152	12.51	9.9864	
2.5×10^{-3}	7.4704		7.470	11.269		9.2951	9.295
4.0×10^{-3}	6.4296	6.430		9.6281	9.628	8.8020	
5.0×10^{-3}	6.0015		6.002	8.9433		7.4937	7.494
7.0×10^{-3}	5.4301	5.430		8.0145		6.7881	
1.0×10^{-2}	4.9161	4.916	4.917	7.1553	7.155	6.1482	6.149
2.0×10^{-2}	4.1724	4.172		5.8147	5.818	5.1984	
4.0×10^{-2}	3.7689	3.769		4.8668	4.867	4.6213	
7.0×10^{-2}	3.6688	3.669		4.3674	4.367	4.4162	
1.0×10^{-1}	3.6581	3.658		4.1556	4.156	4.3748	
2.0×10^{-1}	3.6568	3.657		3.9063	3.906	4.3637	
4.0×10^{-1}	3.6568	3.657		3.7816	3.782	4.3636	
7.0×10^{-1}	3.6568	3.657		3.7281	3.723	4.3636	
1.0	3.6568	3.657		3.7067	3.707	4.3636	
2.0	3.6568	3.657		3.6804	3.682	4.3636	
$+\infty$	3.65680	3.65679		3.65680	3.65679	4.3636	

* Kooijman, 1973.
** Worsoe-Schmidt, 1967.

largest error arises when $Sh_w = 4.0$ and the boundary film is fully developed, where $Sh_\infty = 4.0$, thus from Eq. 21 $Sh_{avg,z,0} = 2.0$, but the calculated value of $Sh_{avg,z,0}$ according to Kooijman's suggestion is 1.91, and the error is 4.5%, which means that for a given C' the error of the calculated z' is 4.5 % according to Eq. 20. These errors are not quite large when compared to the experimental errors in chemical processes. Nevertheless, for further application in the next section and in succeeding articles, a set of correlations is suggested to obtain more accurate values of Sh_z and $Sh_{avg,z}$ as a function of z' and Sh_w. In Figure 2a, Sh_z and $Sh_{avg,z}$ are given as a function of the dimensionless distance z' for several values of Sh_w, and in Figure 2b, comparison is made with the Sherwood numbers when $Sh_w = +\infty$. We can see in Figure 2a that at the entrance region ($z' \leq 0.01$), the relationship between z' and $Sh_{avg,z}$ (or Sh_z) on the double logarithm coordinate is linear. Thus $Sh_{avg,z}$ can be expressed as

$$Sh_{avg,z} = \alpha z'^{\beta} \tag{43}$$

$$Sh_z = \alpha' z'^{\beta'}. \tag{44}$$

The exponent β (or β') is different for different values of Sh_w, otherwise the lines in Figure 2b should be horizontal, when z' is small.

The lumen Sherwood numbers for different Sh_w when the lumen concentration boundary is fully developed are shown

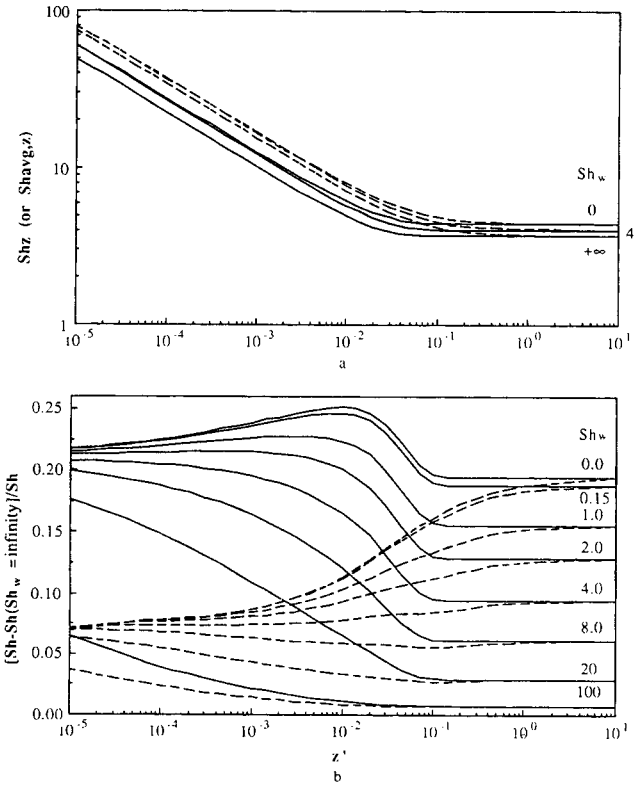

Figure 2. (a) Local and local average lumen Sherwood number as functions of z' and Sh_w; (b) local and average lumen Sherwood numbers for: different Sh_w vs. Sh_w tending to infinity.

Solid lines are for $Sh_{avg,z}$ and dashed lines are for Sh_z.

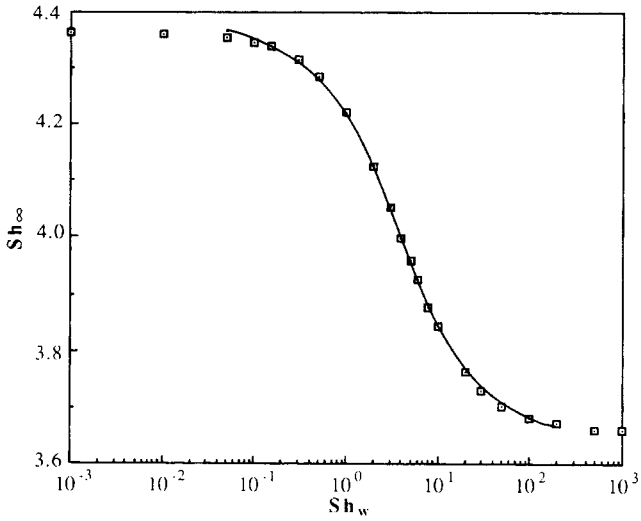

Figure 3. Lumen Sherwood numbers as function of Sh_w when z' tends to infinity.

Points are the calculated values from solving Eqs. 1-4, while the curve represents the regression values.

in Figure 3. A correlation for the calculated values when $0.05 \leq Sh_w \leq 200$ with an average error of 0.065% and a maximum error of 0.2% is obtained as

$$Sh_\infty = -0.2882 \operatorname{arctg}\{-1.555[\log(Sh_w) - 0.583]\} + 4.010. \tag{45}$$

When $Sh_w \leq 0.05$, $Sh_\infty = 4.3636$ with an error of less than 0.1%, and when $Sh_w \geq 200$, $Sh_\infty = 3.6568$ with an error of less than 0.1%.

The following correlation is suggested to express $Sh_{avg,z}$ as a function of Sh_w and z':

$$Sh_{avg,z} = \left[(\alpha z'^{\beta})^{\gamma} + Sh_\infty^{\gamma}\right]^{1/\gamma}. \tag{46}$$

For the entrance region Eq. 46 reduces to Eq. 43. In Eq. 46, γ is treated as a constant, and α and β are treated as a function of Sh_w. For each Sh_w, more than 240 points, uniformly distributed on the logarithm coordinate of z' from 10^{-5} to 10, were used to get the best values for α, β, and γ. The best fit of γ for all the values of Sh_w is 3.65 ± 0.07; and the values of α and β for various Sh_w are shown in Figure 4. The data can be correlated by the following equations. When $0.1 \leq Sh_w \leq 1{,}000$

$$\alpha = 1.608 - 5.874\times10^{-2}\log(Sh_w) - 6.94\times10^{-2}\log^2(Sh_w) + 1.459\times10^{-3}\log^3(Sh_w) + 2.314\times10^{-2}\log^4(Sh_w) - 5.285\times10^{-3}\log^5(Sh_w) \qquad R^2 = 0.999 \tag{47}$$

$$\beta = -0.3387 - 3.871\times10^{-3}\log(Sh_w) - 4.014\times10^{-3}\log^2(Sh_w) + 5.779\times10^{-4}\log^3(Sh_w) + 1.480\times10^{-3}\log^4(Sh_w) - 3.798\times10^{-4}\log^4(Sh_w) \qquad R^2 = 0.992. \tag{48}$$

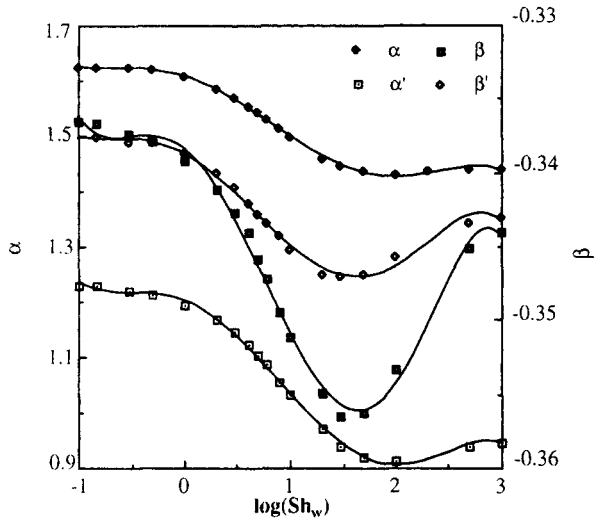

Figure 4. Empirical parameters in Eqs. 43 and 44 as a function of Sh_w.

Points are the calculated values from solving Eqs. 1-4, while the curve represents the regression values.

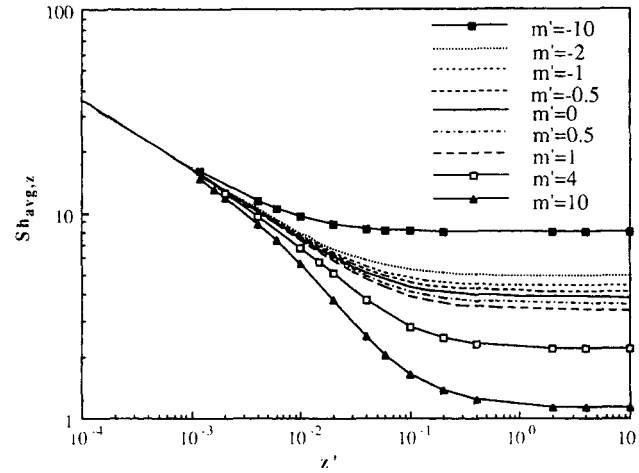

Figure 5. Typical variation of local average Sherwood number $Sh_{avg,z}$ with z' using separation factors m' as a parameter ($Sh_w = 10$).

When $Sh_w \le 0.1$, $\alpha = 1.625$, $\beta = -0.338$, and when $Sh_w \ge 1{,}000$, $\alpha = 1.441$, $\beta = -0.3426$.

For the data of $Sh_{avg,z}$ covering the ranges $0 \le Sh_w \le +\infty$ and $10^{-5} \le z' \le 10$, the average error is 0.17% and the maximum error is 0.58%, or a smaller error for $Sh_{avg,0,z}$ according to Eq. 21. As a comparison to the calculation of $Sh_{avg,0,z}$ at the entrance region ($z' \le 0.01$) for $0 \le Sh_w \le +\infty$, the maximum error of Leveque's equation is 5.8%, that of the correlation of Yang and Cussler (1986) is 7.3%, while that of Urtiaga and Irabien's (1993) is 12.4%.

With an average error of 0.45% and a maximum error of 1.9% the local lumen Sherwood number Sh_z can be expressed as

$$Sh_z = \left[(\alpha' z'^{\beta'})^{5.1} + Sh_\infty^{5.1} \right]^{1/5.1}, \qquad (49)$$

where

$$\alpha' = 1.203 - 7.574\times10^{-2}\log(Sh_w) - 1.138\times10^{-1}\log^2(Sh_w) - 1.449\times10^{-2}\log^3(Sh_w) + 4.546\times10^{-2}\log^4(Sh_w) - 9.462\times10^{-3}\log^5(Sh_w) \qquad R^2 = 0.998 \quad (50)$$

$$\beta' = -0.3384 - 5.522\times10^{-3}\log(Sh_w) - 9.707\times10^{-3}\log^2(Sh_w) - 8.020\times10^{-4}\log^3(Sh_w) + 4.591\times10^{-3}\log^4(Sh_w) - 1.038\times10^{-3}\log^5(Sh_w). \qquad R^2 = 0.993. \quad (51)$$

When $Sh_w \le 0.1$, $\alpha' = 1.2311$, $\beta' = -0.337$, and when $Sh_w \ge 1{,}000$, $\alpha' = 0.9538$, $\beta' = -0.3416$.

Lumen mass-transfer coefficient for Case B

Influence of m' on Lumen Mass-Transfer Coefficient. The influence of the separation factor m' on Sh_z or $Sh_{avg,z}$ is illustrated in Figures 5 and 6, respectively. When z' is large ($> 10^{-3}$), Sh_z and $Sh_{avg,z}$ are significantly influenced by the variation of m', and this influence becomes more pronounced when the lumen film boundary is fully developed (i.e., Sh_z and $Sh_{avg,z}$ tend to a constant). Sh_z and $Sh_{avg,z}$ increase with an increase in mQ_l/Q_s for the countercurrent mode, while Sh_z and $Sh_{avg,z}$ decrease with an increase of mQ_l/Q_s for the cocurrent mode. Thus, compared to the cocurrent mode, the countercurrent mode not only provides a higher logarithmic mean driving force, but also provides a higher lumen mass-transfer coefficient for the given value of mQ_l/Q_s. To the best of our knowledge, this significant phenomenon has never been noticed before for shell-and-tube heat or mass-transfer devices.

Another interesting phenomenon found is that when the countercurrent mode is adopted with $mQ_l/Q_s = 1$, Sh_∞ is 4.3636, whatever the value of Sh_w is (see Figure 6). This can

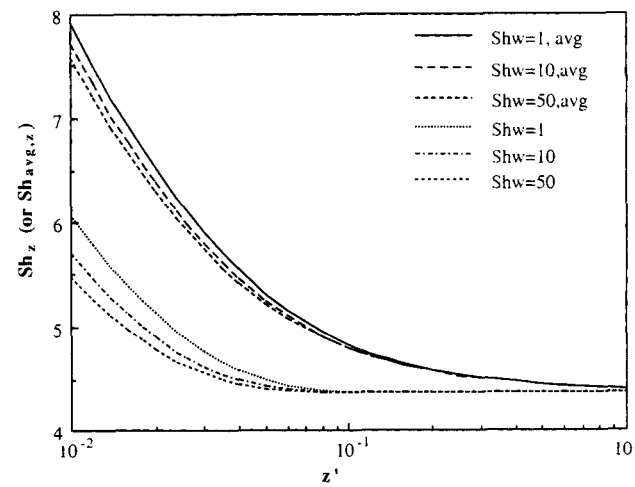

Figure 6. Typical variation of local Sherwood number Sh_z and local average Sherwood number $Sh_{avg,z}$ with z' for various Sh_w when $m' = -1$.

be explained by (1) if the lumen concentration is C_0, the shell outlet mixed-cup concentration is $C_{s,Z}$, and the lumen mixed-cup concentration is C_z at a given z, then the shell bulk concentration is $C_{s,Z}-[Q_l/Q_s\ (C_0-C_z)$. Thus the overall concentration difference is $C_z-[mC_{s,Z}-m(Q_l/Q_s)(C_0-C_z)]=C_0-mC_{s,Z}$, which means that the overall concentration difference along the module is constant; (2) when the lumen concentration boundary is fully developed, Sh_z and $Sh_{\text{avg},z}$, and thus, $Sh_{\text{avg},0,z}$ and $K_{\text{avg},0,z}$, tend to be constant. As a result, the mass flux through the membrane, the product of overall mass-transfer coefficient and the overall concentration difference, is a constant for a large z' value. Therefore, it is reasonable that when $m'=-1$ and $z'\to+\infty$, Sh_z or $Sh_{\text{avg},z}$ tends to the value for the case of constant flux through the wall.

An attempt was made to find a rule for the variation of the fully developed Sherwood number Sh_∞ with m'. As shown in Figure 7, when $-5\le m'\le 2$, Sh_∞ varies strictly linearly with m' for a certain Sh_w. This makes the prediction of Sh_∞ at a given m' very easily, because each line passes through two special points: $(-1,4.364)$ and $[0,Sh_\infty(Sh_w)]$ in Figure 7. Therefore $Sh_\infty(Sh_w,m')$ can be expressed as

$$Sh_\infty(Sh_w,m')=m'[Sh_\infty(Sh_w)-4.364]+Sh_\infty(Sh_w). \quad (52)$$

It can be seen in Figure 7 that the higher the value of Sh_w, the more pronounced the influence of m', and when Sh_w is small, the effect of m' can be negligible. This actually reflects the influence of the variation of shell concentration along the axial direction of the modules on the lumen mass transfer.

For conventional absorption/desorption processes, the absorption factor is usually from 0.7 to 1.4, and for conventional extraction/stripping processes, the extraction factor is usually from 1 to 5 (Perry and Green, 1984). Thus the data of Sh_∞ beyond $-5\le m'\le 2$ are not further correlated.

We can conclude that m' affects the lumen mass-transfer coefficient in a larger degree than Sh_w does, for example, the largest error for Case A is 4.5%, as discussed in the previous section, but this error can be introduced by $m'=\pm 0.23$ for large Sh_w when z' is large.

The following correlations are used to predict $Sh_{\text{avg},z}$ and Sh_z for the set of Sh_w, z' and m':

$$Sh_{\text{avg},z}(Sh_w,m')=\left[(\alpha\, z'^{\beta})^{3.65}+Sh_\infty(Sh_w,m')^{3.65}\right]^{1/3.65} \quad (53)$$

$$Sh_z(Sh_w,m')=\left[(\alpha' z'^{\beta'})^{5.1}+Sh_\infty(Sh_w,m')^{5.1}\right]^{1/5.1}. \quad (54)$$

The value of α, β', α', β' is the same as obtained before. The maximum error of $Sh_{\text{avg},z}(Sh_w,m')$ and $Sh_z(Sh_w,m')$ is 0.72% for the range of $0\le Sh_w\le+\infty$ when $-1\le m'\le 0$; it is 4.2% when $-5\le m'\le -1$; and when $0<m'\le 4$, it is 12.2% for high values of Sh_w.

Proofs from the Literature. The effect of the flow mode of the shell fluid on the lumen mass transfer has hardly been studied. One reason for this is that the hollow-fiber modules of laboratory scale are usually short (then a small z'), thus making the *shell effect* negligible. Furthermore, when the resistance of the membrane wall and/or shell fluid is dominant, that is, Sh_w is small, the effect of m' is small, which makes an accurate calculation of the lumen mass-transfer coefficient unnecessary. Besides, no researcher realized this effect and intentionally performed such an experiment. Nevertheless, a few examples can be found indicating that the experimental data of the overall mass-transfer coefficient in the countercurrent mode are systematically higher than those in the cocurrent mode (D'Elia et al., 1986, Fig. 3; Tai et al., 1994, Fig. 3.), which is the same conclusion obtained here.

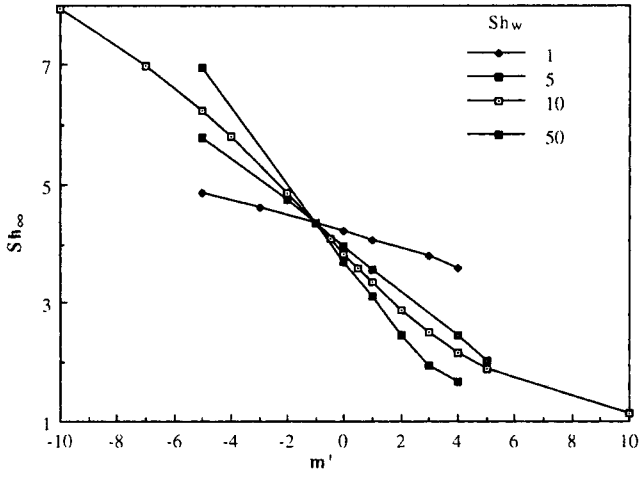

Figure 7. Typical variation of lumen local Sherwood number when $Z'\to\infty$ with separation factor with Sh_w as a parameter.

Experimental results

In order to demonstrate the influence of the cocurrent or countercurrent mode on the mass transfer in the lumen side, experiments were performed where ammonia was desorbed from an aqueous solution in the lumen through a gas membrane supported in the porous wall to pure water in the shell. According to Eqs. 40–42, the logarithm of $C_0(t)-mC_{s,0}(t)$ varies linearly with time, allowing $K_{\text{avg},Z,0}$ or $Sh_{\text{avg},Z,0}$ to be determined from the slope. The value of $Sh_{\text{avg},z,0}$ under various experimental conditions is shown in Figures 8 and 9. We can see that in all cases the values of $Sh_{\text{avg},z,0}$ in the countercurrent mode are systematically higher than those obtained for the cocurrent mode, as obtained from mathematical model simulation. The difference is certainly not from the experimental error, since the maximum experimental error of the value of $Sh_{\text{avg},Z,0}$ is 3%, obtained as the average value for thrice repeated experiments under the same conditions. As in Figure 8, a difference of more than 10% for $Sh_{\text{avg},Z,0}$ can be observed when $mQ_l/Q_s=1$, or a higher difference for $Sh_{\text{avg},Z}$ according to Eq. 21. As can be seen in Figure 8, for a given value of u, and thus a certain value of Z', a higher value of $|m'|$ does not produce a more significant difference between the values of $Sh_{\text{avg},Z,0}$ in the countercurrent mode and those in the cocurrent mode, since in this case, the increase of $|m'|$ is obtained by fixing the lumen flow rate while decreasing the shell flow rate. As indicated by the correlations of the shell mass-transfer coefficients in the literature (Costello et al., 1993), the shell mass-transfer coefficient

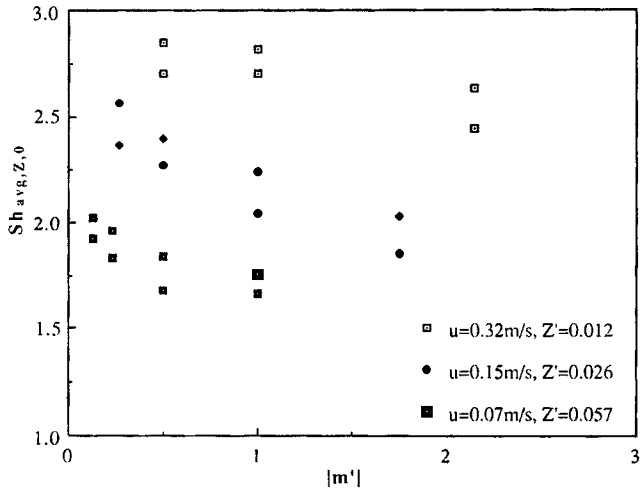

Figure 8. Overall average Sherwood number under various experimental conditions, $T = 45°C$, for each group of data.

The points above are by countercurrent mode, the points below are by cocurrent mode.

varies with the $0.5 \sim 1.0$ power of the shell flow rate, and as a result, Sh_w decreases. In Figure 8 it can also be seen that for a given value of m', for example, $|m'| = 1$, the decrease in shell resistance by an increase in Q_s does not significantly increase the difference in $Sh_{\text{avg},Z,0}$ for the two operational modes, because the simultaneous increase in Q_l reduces the value of Z', thus decreasing the effect of m', as concluded before.

As an alternative, another attempt to modify the value of m' was to change m, for which the salting-out effect was used. The variation of the solubility of ammonia with salt concentration can be expressed as (Hermann et al., 1995)

$$\log(m) = KC_{\text{salt}}, \tag{55}$$

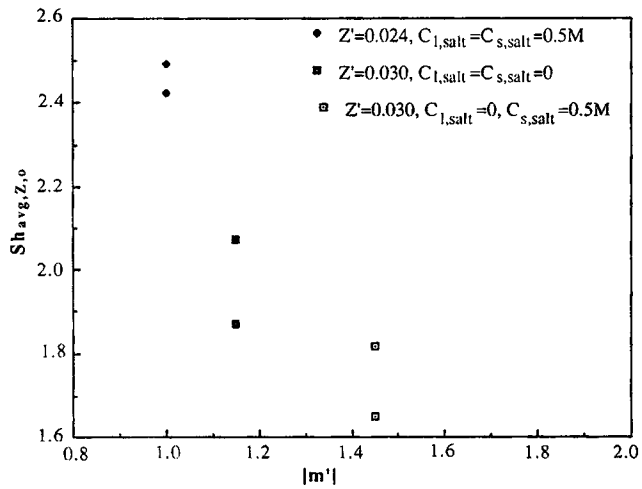

Figure 9. Overall average Sherwood number under various experimental conditions, $T = 25°C$, $u = 0.10$ m/s, for each group of data.

The points above are by countercurrent mode, the points below are by cocurrent mode.

where m is the ratio of the solubility of ammonia in pure water to the solubility of ammonia in a salt-containing solution at a certain ammonia partial pressure; C_{salt} is the salt concentration; and K is the Sechenov constant. If a pure aqueous solution flows through the lumen and an aqueous salt-containing solution flows through the shell, m is exactly as defined before the phase equilibrium coefficient of the component between the lumen and shell fluids. Due to its high value of K (Hermann et al., 1995), Na_2SO_4 was used in the experiments. When the salt concentration is 0.5 M, $m = 1.25$. As can be seen in Figure 9, the addition of salt does not significantly increase the $Sh_{\text{avg},Z,0}$ difference for the two operational modes. However, on the whole, the values of $Sh_{\text{avg},Z,0}$ significantly decrease, because the addition of 0.5 M Na_2SO_4 at 25°C changes the viscosity of water from 0.89 to 1.14 mPa·s, and consequently, the diffusion coefficient of ammonia in the shell solution, and thus Sh_w, decreases. When the same salt concentration is simultaneously added to the feed in the lumen, $m = m_l m_s = 1$, while the mass-transfer coefficient through the membrane increases by a factor of m_l. The higher viscosity results in a lower diffusion coefficient in the lumen, and thus a lower z', and in the shell the higher viscosity also results in a lower mass transfer coefficient. As a net result, the value of $Sh_{\text{avg},Z,0}$ increases, but their difference does not increase as in Figure 9.

Conclusion

Among the applications of hollow-fiber membrane processes, there are some cases in which the membrane-permeating component is diluted in the lumen fluid. These can be found in new membrane processes under development. In these cases, the flux through the membrane is small, and thus the volumetric flow rate of the two fluids, unlike in the traditional membrane processes, can be taken as constant. When a constant external (wall and shell) resistance and a constant shell concentration are present, the boundary conditions are linear. In this article, by numerically solving the continuity mass conservation equation with the linear boundary conditions, we obtained and correlated the lumen Sherwood number as a function of the dimensionless parameters Sh_w and z'. The correlations greatly improve the calculated accuracy of the overall mass-transfer coefficient, and can be used to obtain the lumen mixed-cup concentration by a set of algebraic equations instead of the partial differential equation. The correlations also provide a basis for calculating the lumen mass-transfer coefficient when a more complicated boundary condition occurs at the lumen surface.

Countercurrent contacting is often used to give a better separation in many unit operations in the chemical industry, and it is usually understood that countercurrent contacting provides a higher average mass-transfer driving force than does cocurrent contacting. In many membrane separations, one flow is in excess, so that the type of contacting is not important. Yet there are many hollow-fiber applications in which excess feed or excess stripping fluid cannot be used, and thus, the shell concentration may vary along the axial direction. Therefore, in this article a case is studied where the external resistance is constant, but where the shell concentration varies along with the axial direction resulting from the operational cocurrent or counter-current mode. The sep-

aration factor m' is used to characterize this effect. The numerical calculation results demonstrate that the lumen Sherwood number is independent of the real lumen and shell concentrations, but it is a function of m' as well as Sh_w and z'. And this effect becomes more pronounced when Sh_w and/or z' are large. The countercurrent mode, when compared to the cocurrent mode, not only provides a higher driving force but also provides a higher lumen mass-transfer coefficient. The preceding conclusion is supported by the experimental data in literature and the SGM experimental data in the present article. On the basis of solving the continuity mass conservation equation with the boundary conditions, the lumen Sherwood number is obtained and correlated as a function of Sh_w, z', and m'. The correlations can be used to obtain the lumen mixed-cup concentration by a set of algebraic equations, which are used instead of partial differential equations with more accuracy compared to that described in literature.

These results can be used for the analogous tube-shell laminar heat or mass-transfer processes as well. To the best of our knowledge, this is the first theoretical analysis of the effect of the shell concentration (temperature) variation on the lumen (thus, the overall) mass (heat) -transfer coefficients.

Acknowledgments

The authors are grateful to Prof. D. M. Prazeres for his helpful suggestions and stimulating discussions.

Notation

C = concentration of the component in lumen fluid of the hollow-fiber module, M
C' = dimensionless concentration of the component in fiber lumen
C_0 = inlet concentration of the component in the lumen at the fiber entrance or the bulk concentration of the component in the lumen-side reservoir, M
$C_0(0)$ = initial concentration of the component in the lumen-side reservoir, M
$C_0(t)$ = concentration of the component in the lumen-side reservoir at time t, M
$C_{m,s}$ = concentration of the component in the shell fluid at the fiber outside surface, M
C_R = concentration of the component in the lumen fluid at the lumen surface, M
C'_R = dimensionless concentration of the component in the lumen fluid at the lumen surface
C_s = shell bulk concentration of the component when the concentration is constant, M
$C_{s,0}$ = inlet concentration of the component in the shell or the bulk concentration of the component in the shell-side reservoir, M
$C_{s,0}(O)$ = initial concentration of the component in the shell-side reservoir, M
$C_{s,0}(t)$ = concentration of the component in the shell-side reservoir at time t, M
$C_{s,z}$ = mixed-cup concentration of the component in the shell at z, M
C_z = mixed-cup concentration of the component in fiber lumen at z, M
D = molecular diffusion coefficient of the component in lumen fluid, m^2/s
k_m = mass-transfer coefficient through the membrane (based on the lumen radius), m/s
k_s = mass-transfer coefficient through the shell (based on the lumen radius), m/s
K = external (membrane wall and shell side) mass-transfer coefficient of the component (based on the lumen radius), m/s
$K_{avg,z}$ = average lumen film transfer coefficient from the entrance to z, m/s
$K_{avg,Z,0}$ = average overall mass-transfer coefficient of the module, m/s
K_z = local lumen film transfer coefficient at z, m/s
$K_{z,0}$ = local overall film transfer coefficient at z, m/s
m_l = phase equilibrium coefficient of the component between the lumen fluid and membrane
m_s = phase equilibrium coefficient of the component between the membrane and shell phases
r = radial coordinate, m
r' = dimensionless radius coordinate
R = fiber lumen radius, m
Q_l = total volumetric flow rate through lumen of the module, m^3/s
Q_s = total volumetric flow rate through shell of the module, m^3/s
Sh_∞ = Sherwood number when $z' \to +\infty$
$Sh_{avg,Z,0}$ = Sherwood number based on $K_{avg,Z,o}$
u = average velocity in the lumen, m/s
z = axial coordinate, m
z' = dimensionless axial coordinate
Z = effective length of the module, m
Z' = dimensionless length of the module

Literature Cited

Al-Saffar, H. B., J. S. Oklany, B. Ozturk, and R. Hughes, "Removal of Carbon Dioxide from Gas Streams using a Gas/Liquid Hollow Fiber Module," *Ind. Chem. Eng.*, **73**, 144 (1995).

Basu, R., and K. K. Sirkar, "Pharmaceutical Product Recovery Using a Hollow Fiber Contained Liquid Membrane: A Case Study," *J. Memb. Sci.*, **75**, 131 (1992).

Brookes, P. R., and A. G. Livingston, "Aqueous – Aqueous Extraction of Organic Pollutants Through Tubular Silicone Rubber Membranes," *J. Memb. Sci.*, **104**, 119 (1995).

Cooney, D. O., S. S. Kim, and E. J. Davis, "Analysis of Mass Transfer in Hemodialyzers for Laminar Blood Flow and Homogeneous Dialysate," *Chem. Eng. Sci.*, **29**, 1731 (1974).

Costello, M. J., A. G. Fane, P. A. Hogan, and R. W. Schofield, "The Effect of Shell Side Hydrodynamics on the Performance of Axial Flow Hollow Fibre Modules," *J. Memb. Sci.*, **80**, 1 (1993).

Dahuron, L., and E. L. Cussler, "Protein Extractions with Hollow Fibers," *AIChE J.*, **34**, 130 (1988).

D'Elia, N. A., L. Dahuron, and E. L. Cussler, "Liquid-Liquid Extractions with Microporous Hollow Fibers," *J. Memb. Sci.*, **29**, 309 (1986).

Finlayson, B. A., *Nonlinear Analysis in Chemical Engineering*, McGraw-Hill, New York, p. 73 (1980).

Haan, A. B., P. V. Bartels, and J. Graauw, "Extraction of Metal Ions from Waste Water. Modelling of the Mass Transfer in a Supported-liquid-membrane Process," *J. Memb. Sci.*, **45**, 281 (1989).

Hermann, C., I. Dewes, and A. Schumpe, "The Estimation of Gas Solubilities in Salt Solutions," *Chem. Eng. Sci.*, **50**, 1673 (1995).

Hutter, J. C., G. F. Vandegrift, L. Nuñez, and D. H. Redfield, "Removal of VOCs from Groundwater Using Membrane-assisted Solvent Extraction," *AIChE J.*, **40**, 166 (1994).

Karoor, S., and K. K. Sirkar, "Gas Absorption Studies in Microporous Hollow Fiber Membrane Modules," *Ind. Eng. Chem. Res.*, **32**, 674 (1993).

Kooijman, J. M., "Laminar Heat or Mass Transfer in Rectangular Channels and in Cylindrical Tubes for fully Developed Flow: Comparison of Solutions Obtained for Various Boundary Conditions," *Chem. Eng. Sci.*, **28**, 1149 (1973).

Kreulen, H., C. A. Smolders, G. F. Versteeg, and W. P. M. Van Swaaij, "Microporous Hollow Fiber Membrane Modules as Gas-Liquid Contactors. Part 2. Mass Transfer with Chemical Reaction," *J. Memb. Sci.*, **78**, 217 (1993).

Li, K., D. R. Acharya, and R. Hughes, "Removal of Carbon Dioxide from Breathing Gas Mixtures using a Hollow-fiber Permeators," *Gas Sep. Purif.*, **4**, 197 (1990).

Nii, S., H. Takeuchi, and K. Takahashi, "Removal of CO_2 by Gas Absorption across a Polymeric Membrane," *J. Chem. Eng. Jpn.*, **25**, 67 (1992).
Perry, R. H., and D. W. Green, *Perry's Chemical Engineers' Handbook*, 6th ed., McGraw-Hill, New York (1984).
Prasad, R., and K. K. Sirkar, "Dispersion-free Solvent Extraction with Microporous Hollow Fibers Modules," *AIChE J.*, **34**, 177 (1988).
Prasad, R., and K. K. Sirkar, "Hollow Fiber Solvent Extraction: Performances and Design," *J. Membr. Sci.*, **50**, 153 (1990).
Qin, Y. J., J. M. S. Cabral, and S. C. Wang, "Hollow Fiber Gas-Membrane Process for Removal of NH_3 from Solution of NH_3 and CO_2," *AIChE J.*, **42**, 1945 (1996).
Qin, Y. J., and J. M. S. Cabral, "Hollow Fiber Supported Liquid-Membrane Separation Process for the Separation of NH_3 from Aqueous Media Containing NH_3 and CO_2," *J. Chem. Technol. Biotechnol.*, **65**, 137 (1996).
Qin, Y. J., and J. M. S. Cabral, "Improvement on the Design of Hollow Fiber Separators," in press (1997).
Raghunath, R., and S. T. Hwang, "General Treatment of Liquid-phase Boundary Layer Resistance in the Pervaporation of Dilute Aqueous Organics through Tubular Membranes," *J. Memb. Sci.*, **75**, 29 (1992).
Saito, K., K. Uezu, T. Hori, and S. Furusaki, "Recovery of Uranium from Seawater Using Amidoxime Hollow Fibers," *AIChE J.*, **34**, 411 (1988).
Sarti, G. C., C. Gostoli, and S. Bandini, "Extraction of Organic Components from Aqueous Streams by Vacuum Membrane Distillation," *J. Memb. Sci.*, **80**, 21 (1993).
Tai, M. S. L., I. Chua, K. Li, W. J. Ng, and W. K., Teo, "Removal of Dissolved Oxygen in Ultrapure Water Production using Microporous Membrane Modules," *J. Memb. Sci.*, **87**, 99 (1994).
Takeuchi, H., K. Takahashi, and M. Nakano, "Mass Transfer in Single Oil-containing Microporous Hollow Fiber Contactors," *Ind. Eng. Chem. Res.*, **29**, 1476 (1990).
Tang, E. T., and S.-T. Hwang, "Mass Transfer of Dissolved Gases through Tubular Membrane," *AIChE J.*, **22**, 1,000 (1976).
Tompkins, C. J., A. S. Michaels, and S. W. Peretti, "Removal of p-Nitrophenol from Aqueous Solution by Membrane-Supported Solvent Extraction," *J. Membr. Sci.*, **75**, 277 (1992).
Urtiaga, A. M., M. I. Ortiz, E. Salazar, and J. A. Irabien, "Supported Liquid Membranes for the Separation-Concentration of Phenol. 1. Viability and Mass-Transfer Evaluation," *Ind. Eng. Chem. Res.*, **31**, 877 (1992).
Urtiaga, A. M., and J. A. Irabien, "Internal Mass Transfer in Hollow Fiber Supported Liquid Membranes," *AIChE J.*, **39**, 521 (1993).
Wang, K. L., S. C. McCray, D. D. Newbold, and E. L. Cussler, "Hollow Fiber Air Drying," *J. Memb. Sci.*, **72**, 231 (1992).
Wang, K. L., and E. L. Cussler, "Baffled Membrane Made with Hollow Fiber Fabric," *J. Memb. Sci.*, **85**, 265 (1993).
Wang, S. C., S. C. Xu, and Y. J. Qin, "Mass Transfer in Membrane Absorption-Desorption of Ammonia from Ammonia Water," *Chin. J. Chem. Eng.*, (English Ed.), **1**, 160 (1993).
Worsoe-Schmidt, P. M., "Heat Transfer in the Thermal Entrance Region of Circular Tubes and Annular Passages with Fully Developed Laminar Flow," *Int. J. heat Mass Transfer*, **10**, 541 (1967).
Wu, D. R., S. M. Cramer, and G. Belfort, "Kinetics Resolution of Racemic Glycidyl Butyrate Using a Multiphase Membrane Enzyme Reactor: Experiments and Model Verification," *Biotechnol. Bioeng.*, **41**, 979 (1993).
Yang, M. C., and E. L. Cussler, "Designing Hollow Fiber Contactors," *AIChE J.*, **32**, 1910 (1986).
Yeh, H. M., and C. M. Huang, "Solvent Extraction in Multiphase Parallel-Flow Mass Exchanger of Microporous Hollow-Fiber Modules," *J. Memb. Sci.*, **103**, 135 (1995).
Yi, J., and L. L. Tavlarides, "Modeling Chemically Active Liquid Membranes in Tubular Inorganic Supports," *AIChE J.*, **41**, 1403 (1995).
Yun, C. H., R. Prasad, and K. K. Sirkar, "Membrane Solvent Extraction Removal of Priority Organic Pollutants from Aqueous Waste Streams," *Ind. Eng. Chem. Res.*, **31**, 1709 (1992).
Zhang, Q., and E. L. Cussler, "Microporous Hollow Fibers for Gas Absorption: I. Mass Transfer in the Liquid," *J. Memb. Sci.*, **23**, 321 (1985a).
Zhang, Q., and E. L. Cussler, "Hollow Fiber Gas Membrane," *AIChE J.*, **31**, 1548 (1985b).

Appendix

When metal ion M^{2+} is stripped from an aqueous solution by an MBE or SLM process using chelation acid as the carrier, interfacial reaction can be expressed as (Yi and Tavlarides, 1995):

$$M^{2+}(aq.) + 2HR(or.) = MR_2(or.) + 2H^+(aq.). \tag{A1}$$

When the reaction takes place at high carrier concentration compared to the metal ion concentration, and the pH is maintained constant or the hydrogen-ion concentrations are large compared to the metal ion or metal complex concentrations, the approximations yield interfacial reaction rates of the form of first-order reversible reaction as (Yi and Tavlarides, 1995):

$$R_l = k_l C_{M^{2+},l} - k'_l C_{MR2,m,l} \qquad \text{(at lumen surface)} \tag{A2}$$

$$R_s = k'_s C_{MR_2,m,s} - k_s C_{M^{2+},m,s}$$

(at outside surface, when operated as an SLM process), (A3)

where k and k' are the interfacial rate coefficients at the lumen and lumen interfaces, respectively, l = lumen side, m = membrane surface, and s = shell side.

When it is operated as an MBE process, the boundary condition at the lumen interface is

$$-D\frac{\partial C}{\partial r} = k_l C_{M^{2+},l} - k'_l C_{MR_2,m,l} = k_m(C_{MR_2,m,l} - C_{MR_2,m,s}) = k_s(C_{MR_2,m,s} - C_{MR_2,s}). \tag{A4}$$

Equation (A4) can be arranged as

$$-D\frac{\partial C}{\partial r} = \frac{C_{M^{2+},l} - \frac{k'_l}{k_l}C_{MR_2,s}}{\frac{1}{k_l} + \frac{k'_l}{k_l k_m} + \frac{k'_l}{k_l k_s}}. \tag{A5}$$

Let

$$C' = \frac{C_{M^{2+},l} - \frac{k'_l}{k_l}C_{MR_2,s}}{C_{M^{2+},0} - \frac{k_l}{k_l}C_{MR_2,s}} \tag{A6}$$

$$Sh_w = \frac{2R}{D\left(\frac{1}{k_l} + \frac{k'_l}{k_l k_m} + \frac{k'_l}{k_l k_m}\right)}, \tag{A7}$$

then Eq. (A5) can be reduced to Eq. 15.

When it is operated as an SLM process, the boundary condition at the lumen interface is

$$-D\frac{\partial C}{\partial r} = k_l C_{M^{2+},l} - k'_l C_{MR_2,m,l} = k_m(C_{MR_2,m,l} - C_{MR_2,m,s}) = k'_s C_{MR_2,m,s} - k_s C_{M^{2+},m,s} = k_s(C_{MR_2,m,s} - C_{MR_2,s}) \quad \text{(A8)}$$

Equation A8 can be arranged as

$$-D\frac{\partial C}{\partial r} = \frac{C_{M^{2+},l} - \frac{k_s k'_l}{k_l k'_s} C_{M^{2+},s}}{\frac{1}{k_l} + \frac{k'_l}{k_l K_m} + \frac{k'_l}{k_l k'_s} + \frac{k_s k'_l}{k_l k'_s k_s}}. \quad \text{(A9)}$$

Let

$$C' = \frac{C_{M^{2+},l} - \frac{k_s k'_l}{k_l k'_s} C_{M^{2+},s}}{C_{M^{2+},0} - \frac{k_s k'_l}{k_l k'_s} C_{M^{2+},s}} \quad \text{(A10)}$$

$$Sh_w = \frac{2R}{D\left(\frac{1}{k_l} + \frac{k'_l}{k_l K_m} + \frac{k'_l}{k_l k'_s} + \frac{k_s k'_l}{k_l k'_s k_s}\right)}, \quad \text{(A11)}$$

then Eq. A9 can be reduced to Eq. 15.

When the operation is executed in the cocurrent or countercurrent mode and the shell concentration variation along the axial direction is included, BC3 identical to Eq. 27 can be derived as well, where $m = (k'_l/k_l)$ for MBE and $m = (k_s k'_l/k_l k'_s)$ for SLM, respectively.

Therefore, m is actually the interfacial reaction equilibrium constant at the lumen interface for the MBE case, and m is actually the ratio of the interfacial reaction equilibrium constant at the lumen interface to that at the shell interfacial for the SLM case.

Manuscript received July 19, 1996, and revision received Feb. 18, 1997.

Corrections

- In the article titled "Two-Dimensional Model for Circulating Fluidized-Bed Reactors" (July 1996, p. 1875), the sixth line below Eq. 19 on p. 1880 "Luca et al. (1995)" should be changed to "Marmo et al. (1995)." In addition, the names of authors of "Comparison Among Several Predictive Models for Circulating Fluidized Bed Reactors" in the Literature Cited section (p. 1888) should be changed to "Marmo, L., L. Manna, and G. Rovero" from "Luca, M., M. Luigi, and R. Giorgio."
- In the article titled "High-Energy Density Storage of Natural Gas in Light Hydrocarbon Solutions (April 1997, p. 1108), the captions for Figures 3, 4 and 5 should read "...stored in 21 MPa," not "...stored at 21 MPa." Additionally, in Figure 3 "...vs. CNG" should be changed to "...vs. CNG at 21 MPa."